ELSEVIER

Coordination Chemistry Reviews
159 (1997) 385–396

Tailoring of solid state electrical conductivity and optical electron transfer activation of dioxygen in solution through supramolecular charge-transfer interaction in ion pairs

Horst Kisch

Institut für Anorganische Chemie der Universität Erlangen-Nürnberg, Egerlandstr. 1, D-91058 Erlangen, Germany

Received 22 December 1995

Contents

Abstract

Redoxactive and light-sensitive ion pair complexes of the type $\{A^{2+}[ML_2]^{2-}\}$, wherein A^{2+} is a bipyridinium acceptor and $[ML_2]^{2-}$, M=Ni, Pd, Pt, a planar dithiolene metalate, according to their solid state structure can be divided into two classes. Class I consists of compounds which contain an approximately planar acceptor and which therefore can form mixed stacks of slightly slipped coplanar components. Class II complexes contain a strongly twisted acceptor which gives rise to a chain-like structure in which only each a half of a component can adopt a coplanar arrangement. While application of the Hush–Marcus model reveals that both classes possess the same mean reorganization energy for electron transfer from the dianion to the dication, only for class I compounds does the logarithm of the specific electrical conductivity increase linearly with the free activation energy of this process, as calculated from the energy of the ion pair charge transfer band and the redox potentials. For class II complexes there is no similar relation. Proper selection of the acceptor reduction potential and the central metal allows to tailor optical electron transfer-induced activation of dioxygen in solution. The primary electron transfer step affords the oxidized donor, $[ML_2]^-$, and the reduced acceptor, $A^{\bullet+}$, which reduces dioxygen to superoxide. The latter reaction can compete with back-electron transfer only when the reduction potential of A^{2+} is more negative than −0.6 V. The overall reaction proceeds only in the case of M=Pt,

PII S0010-8545(96)01312-4

suggesting that the photoreactive state has ion pair charge transfer character.

Keywords: Dithiolene metallate; Dioxygen; Tailoring of electron transfer interaction in ion pairs

1. Introduction

Charge transfer complexes play an important role in chemical reactivity since they constitute in many cases the very early interaction between two substrates [1]. In addition, also physical properties like non-linear optical effects [2] or electrical conductivity may strongly depend on degree and nature of the CT interaction [3,4]. While the electrical properties of organic CT complexes are quite well investigated, similar work on inorganic systems is rare. In the former case the complexes were usually obtained by combination of uncharged components and their composition and structure changed when the driving force of electron transfer (ET) from the donor D to the acceptor A was varied through the introduction of different substituents [4]. We therefore thought that the use of charged components may prevent structural changes, since the strong coulomb interaction should be decisive as long as the steric alterations remain small. Accordingly, planar dianionic d^8 metal dithiolenes [5] of the type $[ML_2]^{2-}$ and bipyridinium dications [6], A^{2+}, were selected as components since both are known to experience only minor structural changes upon reversible ET (Fig. 1). Thus, the aim of this work was to find out whether, at approximately constant structural factors, the electrical conductivity in the solid and the photoreactivity in solution may be ultimately tailored by rational variation of the supramolecular CT interaction within these light-sensitive and redoxactive ion pairs. Accordingly the components displayed in Fig. 1 were selected in order to change the driving force of ET (ΔG_{12}, Eq. (1)) over a range of about 0.5 eV [7,8].

$$[ML_2]^{2-} + A^{2+} \rightarrow [ML_2]^{-} + A^{\bullet +} \quad (1)$$

For a given metal like nickel(II), variation of the ligand from $dmid^{2-}$ over $dmit^{2-}$ and dmt^{2-} to mnt^{2-} decreases the donor strength as indicated by the reduction potentials from −0.29 over −0.14 and 0.06 to 0.22 V (vs. SCE, in MeCN), respectively. When the $dmit^{2-}$ ligand is kept constant, substitution of nickel by palladium reduces the donor capability by 0.12 V while platinum has only a slight influence. The acceptor strength of the organic components which can adopt a planar geometry increases from −0.43, −0.42, −0.46 V for the viologens MV^{2+}, CV^{2+}, StV^{2+}, to −0.36, −0.32 and −0.06 V for DQ^{2+}, the diazaphenanthrenium DP^{2+} and the dipyridiniumketone DPK^{2+}, respectively. All of the nonplanar 2,2′-bipyridinium compounds are poorer acceptors as indicated by the reduction potentials of −0.75, −0.66 and −0.56 V measured for MQ^{2+}, BQ^{2+} and PQ^{2+}, respectively.

The few other ion pair complexes of viologens reported in the literature have been summarized recently [9,10].

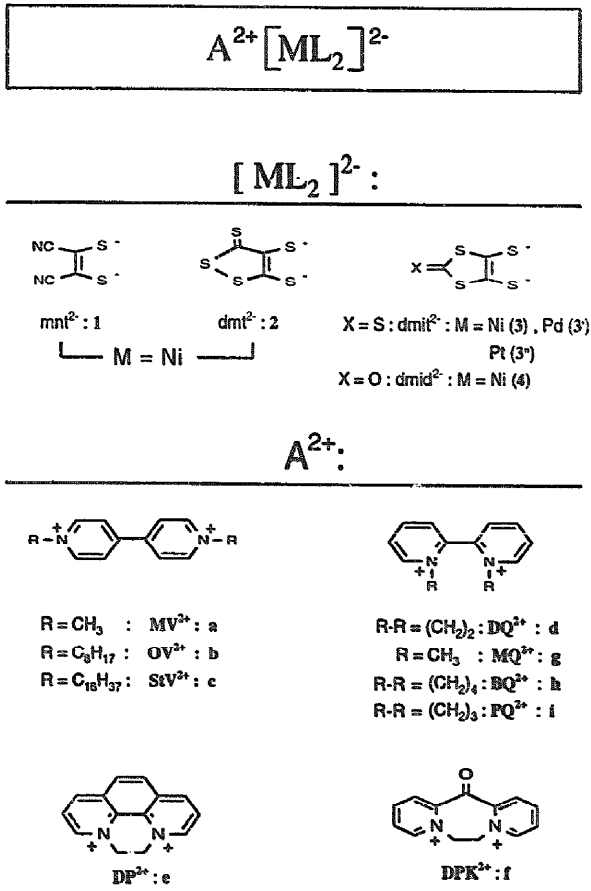

Fig. 1. See text for details.

2. Synthesis and structure

The ion pairs $A[ML_2]$ are easily obtained by metathesis of the tetrabutylammonium dithiolene metalates with the corresponding bipyridinium salts [11–17]. Single crystal X-ray analyses of several ion pairs containing the planar $[M(mnt)_2]^{2-}$ donor revealed the presence of two basic structural types. Class I complexes contain an acceptor which can adopt a planar geometry and the solid-state structure consists of mixed stacks along one crystal axis as illustrated for $MV[Pd(mnt)_2]$ in Fig. 2 [18]. Shortest *intrastack* distances are in the range of 340 pm and occur in this and in the isomorphous nickel homologue between the electron-rich dithiolene sulfur atoms and those viologen carbon atoms (ortho to nitrogen) which carry the highest positive charge [12].

Class II ion pairs contain a nonplanar acceptor and the solid-state structure does not consist of mixed stacks along one crystal axis. This is prevented by the strongly

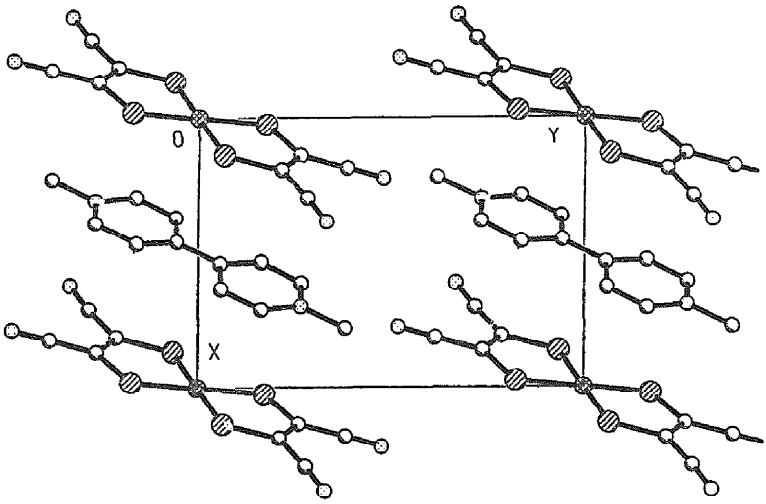

Fig. 2. Solid-state structure of the ion pair MV[Pd(mnt)$_2$].

twisted 2,2′-bipyridinium component which induces a chain-like arrangement as indicated by the structure of BQ[Ni(mnt)$_2$] in Fig. 3 [19]. The two pyridinium rings of BQ^{2+} are twisted by 64° and each of them are coplanar with one half of the dithiolene nickelate. The shortest *interionic* distances are found between the pyridinium nitrogen atom and nickel (356 pm).

In summarizing the structural results, one can conclude from the presently available X-ray data of A[M(mnt)$_2$], M = Ni, Pd, Pt, that in the solid mixed donor–acceptor stacks are formed only when the torsion angle of the bipyridinium acceptor is below 30°, while above this value border line chain-like structures are preferred [20–22].

3. From electron transfer parameters to electrical conductivity

All complexes depicted in Fig. 1 exhibit IPCT bands in the VIS-NIR region of the diffuse reflectance spectrum as exemplified for A[Ni(dmit)$_2$] in Fig. 4. The unusual band of the tetrabutylammonium salt at about 1350 nm has been assigned to an *interligand* π, π^* transition. EHT calculations indicate that the relevant molecular orbitals are localized on both peripheral CS_3 fragments of the $dmit^{2-}$ ligand [17]. This ligand–ligand interaction is not possible when the central metal is a tetrahedral d^{10} ion like Zn(II), as indicated by the absence of this band in the spectrum of $(NBu_4)_2$[Zn(dmit)$_2$].

From Fig. 4 it can be recognized that the good acceptors induce appearance of the IPCT bands in the region of the interligand absorption or at lower energy (Fig. 4(a)), while in the case of the poorer acceptors the bands are displaced to higher energy and may appear only as shoulders (Fig. 4(b)). We therefore used the

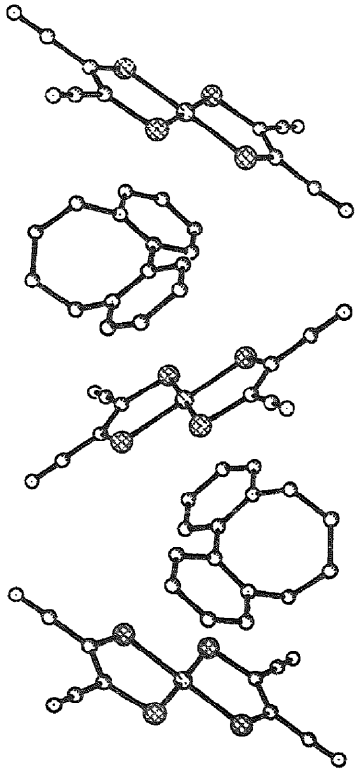

Fig. 3. Solid-state structure of the ion pair BQ[Ni(mnt)$_2$].

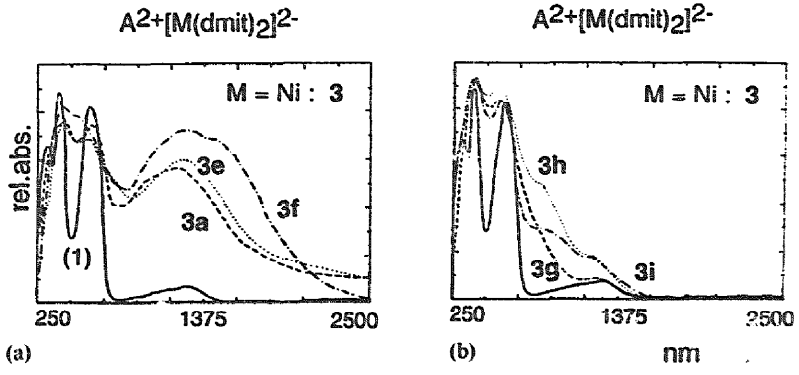

Fig. 4. Diffuse reflectance spectra of $(NBu_4)_2[Ni(dmit)_2]$ (1) as compared to $A[Ni(dmit)_2]$, A^{2+} = MV (3a), DP (3e), DPK (3f), MQ (3g), BQ (3h), PQ (3i).

onset of these bands to determine the energy of optical electron transfer, E_{IPCT}, since the onset is obtainable with higher accuracy than the maximum of the band [23]. As summarized recently, a plot of E_{IPCT} vs. ΔG_{12} for 32 complexes afforded a straight line of the slope 0.9, which is very close to the theoretical value of 1.0 as expected from the Hush-relation, $E_{IPCT}=\chi+\Delta G_{12}$ [9,17,24]. From the intercept, a value of 60 kJ mol^{-1} is obtained for the reorganization energy χ. Thus, one can conclude that for all these ion pairs the basic geometry of the encounter complex of the ET reaction (Eq. (1)) is approximately the same and that changing the driving force shifts only the IPCT energy.

From the above parameters and from the free activation energy, calculated according to $\Delta G^*=(E_{IPCT})^2/4\chi$, a potential energy diagram of the optical ET can be constructed. This is shown in Fig. 5 for the ion pair BQ [Pt(mnt)$_2$] for which ΔG^* is calculated as 117 kJ mol^{-1}. The interaction between the two redox states is small as indicated by the exchange-matrix elements of about 200–400 cm^{-1}, values which are just at the border of the adiabatic limit. Similarly, the calculated fraction, α^2, of an electron transferred in the ground state from $[Pt(mnt)_2]^{2-}$ to A^{2+} is very low, namely in the range of 10^{-4}. These values are typical for outer-sphere complexes and resemble those reported for the $MV^{2+}/[Fe(CN)_6]^{4-}$ ion pair [25].

The fact that the reorganization energy is approximately the same for all ion pairs suggests that changing the driving force ΔG_{12} by the use of different components does not alter the basic structural features, but predominantly controls the amount of charge transferred from $[ML_2]^{2-}$ to A^{2+} in the ground state. This is a prerequisite for a regular influence of ET parameters on the electrical conductivity without interference by steric effects. The value of α^2 is directly proportional to the absorptivity and half band-width of the IPCT band, and indirectly proportional to E_{IPCT} and the square of the distance between the two ions [15,25]. While the two latter values are easily obtainable, this is not the case for the former two due to overlap with other absorption bands. We therefore selected the activation energy ΔG^* as the relevant parameter since the values of E_{IPCT} and χ are available for all complexes. For a series of compounds with similar intercomponent distances and integrated

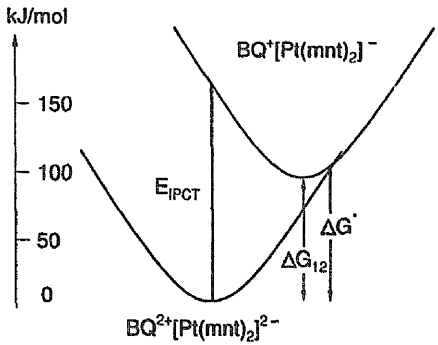

Fig. 5. Relative positions of potential energy curves before and after electron transfer within the ion pair BQ[Pt(mnt)$_2$].

intensities of the IPCT band α^2 increases with decreasing E_{IPCT}. Since ΔG^* decreases upon lowering E_{IPCT} , smaller values of ΔG^* correspond to a higher amount of charge transferred. While for class II compounds the specific electrical conductivity (σ) of pressed powder pellets is almost independent of ΔG^*, a plot of log σ vs. this parameter in the case of class I complexes reveals an approximately linear increase with decreasing ΔG^* (Fig. 6). Although the correlation coefficient of 0.88 is relatively poor, it improves to 0.96 when only the six $[Ni(dmit)_2]^{2-}$ compounds are considered [17]. It is expected that the assumptions made above, the same intercomponent distances and the same intensities of IPCT bands, should be fulfilled rather in a series where one component stays constant.

$$\log \sigma = a + c\Delta G^* \tag{2}$$

The correlation shown in Fig. 6 can be expressed by Eq. (2), wherein a and c are specific constants of class I complexes. It is therefore possible to predict the electrical conductivity quantitatively from an molecular ET parameter. This correlation seems to arise from the fact that, according to the low values of α^2, the CT interaction is orders of magnitudes smaller than the coulomb attraction which seems to determine the donor–acceptor arrangement. Note that the conductivity changes over seven orders of magnitude when the activation energy is varied over a range of 0.5 eV. This suggests that charge generation occurs by ET from the dianion to the anion. Since this process should be enhanced by light absorption, and specially in the spectral region of the IPCT band, the action spectrum of the photoconductivity was measured. In order to avoid interference with MC states, the corresponding d^{10} complexes $A[Zn(mnt)_2]$ were selected. Indeed, photoconductivity maxima were found, red-shifted by about 60 nm to the optical IPCT band [26,27].

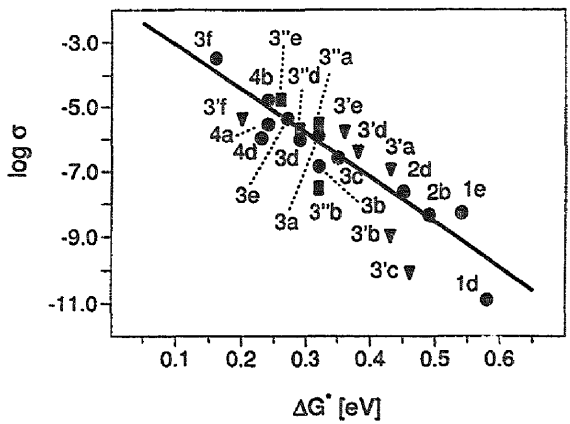

Fig. 6. Plot of the logarithm of the specific electrical conductivity as function of the free activation energy ΔG^* as calculated from the Hush–Marcus model.

4. Optical electron transfer activation of dioxygen

The activation of molecular oxygen is a central topic in basic and applied chemistry. In this process the limiting step is the primary ET to afford the superoxide ion [28]. Since laser flash photolysis [29] revealed that some of the IPCT complexes undergo optical ET (Eq. (3)), we investigated whether the reduced acceptor radical $A^{\bullet+}$ may be able to reduce dioxygen [30,31]. In the case that the monoanion $[Pt(mnt)_2]^-$ could be reduced back to the dianion by an added donor, the ion pair would sensitize the photoreduction of oxygen.

$$\{A^{2+}[Pt(mnt)_2]^{2-}\} + h\nu \rightarrow [Pt(mnt)_2]^- + A^{\bullet+} \quad (3)$$

$$A^{\bullet+} + O_2 \rightarrow A^{2+} + O_2^- \quad (4)$$

$$[Pt(mnt)_2]^- + A^{\bullet+} \rightarrow [Pt(mnt)_2]^{2-} + A^{2+} \quad (5)$$

Continuous irradiation of a series of $A[Pt(mnt)_2]$ complexes in aerated DMSO solution revealed formation of the monoanion $[Pt(mnt)_2]^-$ only in cases when the reduction potential of the acceptor was more negative than about −0.6 V (in DMSO, vs. SCE). This corresponds approximately to the potential necessary to reduce oxygen which, in DMSO solution, amounts to −0.74 V [32]. Therefore it seemed likely that after the primary, optical ET (Eq. (3)) a fast secondary ET to dioxygen (Eq. (4)) prevents back-electron transfer (Eq. (5)), and therefore the monoanion is accumulated.

In order to exclude other mechanistic pathways like a direct ET from the excited IPCT complex, flash photolysis was performed with $[Pt(mnt)_2]^{2-}$ in the presence of reactive and nonreactive acceptors. While in the latter case the second-order recombination of the primary products ($k_{-et} = 5.5 \times 10^9\ M^{-1}\ s^{-1}$, Eq. (5)) is not significantly influenced in aerated solution, the reactive acceptors like MQ^{2+} induce a pseudo first-order decay ($k_2 = 1.9 \times 10^6\ s^{-1}$) of the radical cation $MQ^{\bullet+}$ (Fig. 7). At the same time, the decay of $[Pt[mnt)_2]^-$ becomes slower and does not approach zero. Since the concentration of dioxygen (0.0021 M) is about two orders of magnitude higher than that of $MQ^{\bullet+}$, the pseudo first-order behavior is reasonable. These experimental findings strongly support the proposed mechanism. Furthermore the superoxide ion was scavenged in the presence of the spin trap 5,5-dimethyl-1-pyrroline-*N*-oxide by ESR techniques. No corresponding spin adduct was formed when acceptors of reduction potentials more positive than −0.6 V were employed. UV–VIS reaction spectroscopy indicates that superoxide is transformed to hydrogen peroxide which photochemically reacts with the monoanion to unidentified products.

When platinum is replaced by palladium or nickel, no accumulation of the monoanion can be observed. This can be rationalized when the energy of the relevant excited states, as estimated from the onset of the absorption bands, is considered (Fig. 8). Only in the former case is the IPCT state lowest in energy, while in the two latter cases it is the MC state, either singlet or triplet (Fig. 8). It is likely that the nickel and palladium complexes undergo an efficient radiationless deactivation to the ground state via low-lying triplet states which are not observable in the

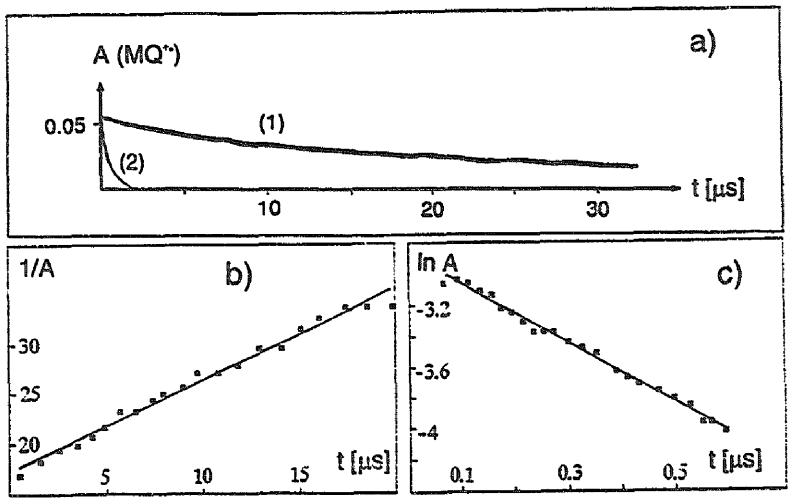

Fig. 7. Laser flash photolysis (λ_{exc}=347 nm) of MQ[Pt(mnt)$_2$] in argon (1) and air (2) saturated DMSO solution; (a) decay of $MQ^{\bullet+}$ measured at λ=380 nm; (b) corresponding second order; (c) first-order kinetic plots.

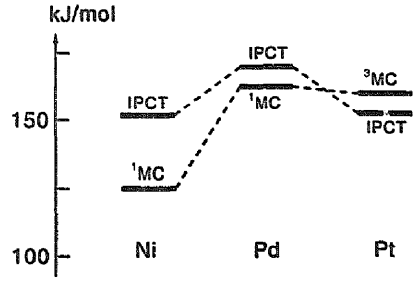

Fig. 8. Energy of lowest excited states for MQ[M(mnt)$_2$], M=Ni, Pd, Pt.

absorption spectrum. The singlet MC state of the platinum complex is located at 220 kJ mol^{-1} [33].

In the continuous irradiation experiments it was found that the quantum yield of monoanion formation in the presence of MQ^{2+} increases from 0.01 to 0.015 and 0.029 when the wavelength of the absorbed light decreases from 580 to 437 and 334 nm, respectively. This dependence can be rationalized when the relative positions of the relevant states are considered (Fig. 9). Using the length of the Pt–S bond as coordinate, the minimum of the IPCT state should be slightly displaced to the left as compared to the ground state since partial oxidation of $[Pt(mnt)_2]^{2-}$ shortens this bond [34]. In the case of the other states Pt–S antibonding orbitals are involved [5b,33] and the minima are displaced to longer Pt–S distances, an effect which should be strongest for the flat potential curve of the MC state. In the resulting arrangement, the parabola of the IPCT state crosses the IL and MLCT curves at

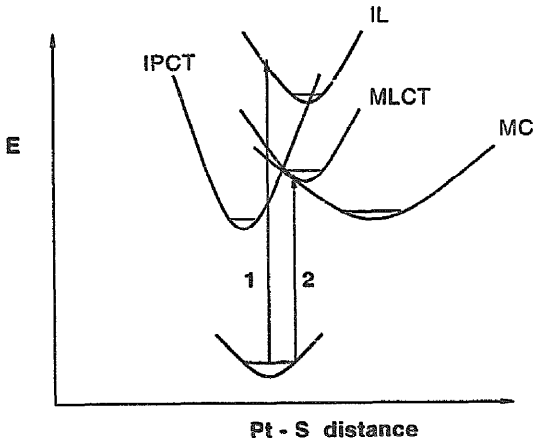

Fig. 9. Consequences of high- and low-energy excitation of MQ[Pt(mnt)$_2$].

their minima, but crosses the MC curve at higher vibrational states. Irradiation at 334 or 437 nm populates the IL in a low and the MLCT state in high vibrational levels. After vibronic relaxation, intersystem crossing to the IPCT state is equally favored. However, since the MLCT state is much closer in energy to the MC state than the IL state, competitive internal conversion to the MC state should occur and the reactive IPCT state becomes less populated. This effect should be stronger upon excitation at 580 nm at which wavelength both the MC and IPCT state are populated.

These experimental findings clearly reveal that the initial step of dioxygen activation is the optical ET within the contact ion pair according to Eq. (3). From the Hush–Marcus model the free activation enthalpy for the *thermal* ET is estimated for the case of BQ[Pt(mnt)$_2$] as 117 kJ mol^{-1}. Since this ion pair is thermally very stable, we tested whether dioxygen activation could be performed also thermally. In fact, while no monoanion is formed when an aerated propylene carbonate solution is heated to 100°C, this occurs at 124–182°C. No monoanion is produced when BQ^{2+} is replaced by tetrabutylammonium as cation. This clearly suggests that the thermal reaction proceeds by the same mechanism as the photoreaction. Assuming a simplified kinetic scheme, k_{et} was obtained for five temperatures by measuring the rate of disappearance of $[Pt(mnt)_2]^{2-}$. The corresponding Arrhenius plot (Fig. 10) affords an activation energy of 108 ± 10 kJ mol^{-1}, which is in excellent agreement with the value of 117 kJ mol^{-1} predicted from the Hush–Marcus model.

5. Summary

The experimental observations presented above clearly reveal that the variation of supramolecular charge-transfer interaction in class I ion pairs which consist of a planar dianionic metal dithiolene and planar bipyridium dication can be used to quantitatively control the solid-state electrical conductivity in a range of seven orders

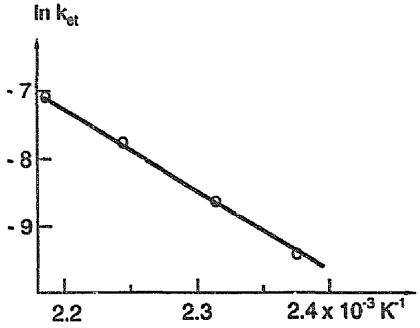

Fig. 10. Arrhenius plot for the rate constant of the thermal electron transfer activation of dioxygen by BQ[Pt(mnt)$_2$] in propylene carbonate at 142–182°C.

of magnitude. This allows the prediction of a solid-state property from a molecular electron transfer parameter, ΔG^*, obtained from the Hush–Marcus theory. Furthermore, a photoinduced electron transfer activation of dioxygen can be tailored by proper selection of the acceptor reduction potential. The primary step of this reaction is an optical electron transfer within the ion pair, followed by reduction of dioxygen to superoxide by the reduced acceptor. Due to the high thermal stability of these compounds, the thermal version of this process also could be realized. The Arrhenius activation energy measured matches the value predicted from the Hush–Marcus model.

Acknowledgements

This work was supported by Deutsche Forschungsgemeinschaft, Volkswagen-Stiftung, and Fonds der Chemischen Industrie. For stimulating cooperation I am thankful to F. Scandola, Ferrara and G. Grampp, Graz.

References

[1] (a) R. Foster, Molecular Association, Academic Press, London, 1979; (b) S. Sankararaman, S. Perrier and J.K. Kochi, J. Am. Chem. Soc., 111 (1989) 6448; (c) J.K. Kochi, Acta Chem. Scand., 44 (1990) 409; (d) R.S. Davidson in R. Foster (ed.) Molecular Association, Academic Press, 1979, London.
[2] H. Sakaguchi, T. Nagamura and T. Matsuo, J. Chem. Commun., (1992) 209.
[3] H.J. Keller and G.Z. Soos, Top. Curr. Chem., 127 (1985) 169.
[4] R.C. Wheland, J. Am. Chem. Soc., 98 (1976) 3926.
[5] (a) G.N. Schrauzer, Adv. Chem. Ser., 110 (1972) 73; (b) J.A. McCleverty, Progr. Inorg. Chem., 10 (1968) 49; (c) E. Hoyer, W. Dietzsch and W. Schroth, Z. Chem., 11 (1971) 41; (d) P.I. Clemenson, Coord. Chem. Rev., 106 (1990) 171.
[6] (a) H. Wolkers, R. Stegmann, G. Frenking, K. Dehnicke, D. Fenske and G. Baum, Z. Naturforsch. Teil B, 48 (1993) 1341; (b) L.A. Summers, The Bipyridinium Herbizides, Academic Press, New York, 1980; (c) E. Weitz, Angew. Chem., 66 (1954) 658.
[7] For recent summaries see Refs. 8–10.

[8] H. Kisch, Coord. Chem. Rev., 125 (1993) 155.
[9] H. Kisch, Comments Inorg. Chem., 16 (1994) 113.
[10] H. Kisch, F. Nüßlein and I. Zenn, Z. Anorgan. Allg. Chem., 600 (1991) 67.
[11] A. Fernandez and H. Kisch, Chem. Ber., 117 (1984) 3102.
[12] H. Kisch, A. Fernandez, Y. Wakatsuki and H. Yamazaki, Z. Naturforsch. Teil B, 40 (1985) 292.
[13] S. Lahner, Y. Wakatsuki and H. Kisch, Chem. Ber., 120 (1987) 1011.
[14] F. Nüßlein, R. Peter and H. Kisch, Chem. Ber. 122 (1989) 1023.
[15] W. Dümler and H. Kisch, Nouv. J. Chem., 15 (1991) 649.
[16] G. Schmauch, F. Knoch and H. Kisch, Chem. Ber. 127 (1994) 287.
[17] I. Nunn, B. Eisen, R. Benedix and H. Kisch, Inorg. Chem. 33 (1994) 5079.
[18] M. Lemke, F. Knoch and H. Kisch, Acta Crystallogr., C49 (1993) 1630.
[19] F. Knoch, G. Schmauch and H. Kisch, Z. Kristallogr., 210 (1995) 76.
[20] F. Knoch, U. Ammon and H. Kisch, Z. Kristallogr., 210 (1995) 78.
[21] M. Lemke, F. Knoch, H. Kisch and J. Salbeck, Chem. Ber., 128 (1995) 131.
[22] G. Schmauch, F. Knoch and H. Kisch, Chem. Ber., 128 (1995) 303.
[23] An extrapolation method avoids errors due to differing amounts of material employed; see B. Karvaly and I. Hevesi, Z. Naturforsch. Teil A, 26 (1971) 245.
[24] (a) N.S. Hush, Progr. Inorg. Chem., 8 (1967) 391; (b) R.A. Marcus and N. Sutin, Comments Inorg. Chem., 5 (1986) 119.
[25] J.L. Curtis, B.P. Sullivan and T.J. Meyer, Inorg. Chem., 19 (1980) 3833.
[26] H. Meier, W. Albrecht, H. Kisch, I. Nunn and F. Nüßlein, Synthetic Metals 48 (1992) 111.
[27] H. Meier, W. Albrecht and H. Kisch, Mol. Cryst. Liqu. Cryst., 217 (1992) 153.
[28] (a) A.E. Martell and D.T. Sawyer, Oxygen Complexes and Oxygen Activation by Transition Metals, Plenum Press, New York and London, 1988; (b) L. Lopez, Top. Curr. Chem., 156 (1990) 117.
[29] H. Kisch, W. Dümler, C. Chiorboli, F. Scandola, J. Salbeck and J. Daub, J. Phys. Chem., 96 (1992) 10323.
[30] U. Ammon, G. Grampp and H. Kisch, J. Inf. Rec. Mats. 21 (1994) 667.
[31] U. Ammon, Ph.D. Thesis, University of Erlangen-Nürnberg, 1995.
[32] D.T. Sawyer and J.L. Robert, J. Electroanal. Chem., 189 (1985) 121.
[33] S.I. Shupack, E. Billig, R.J.H. Clark, R. Williams and H.B. Gray, J. Am. Chem. Soc., 86 (1964) 4594.
[34] S. Alvarez, R. Vicente and R. Hoffmann, J. Am. Chem. Soc., 107 (1985) 6235.